International Journal of Science and Research (IJSR)
ISSN (Online): 2319-7064
Index Copernicus Value (2015): 78.96 | Impact Factor (2015): 6.391

Spectroscopic Studies on Dy^{3+} Ions Doped $NaCaAlPO_4F_3$ Phosphor for Luminescent Applications

R. Nagaraja[1], V. Pushpa Manjari[2], G. Thirumala Rao[3], B. Sailaja[4], R.V.S.S.N. Ravikumar[5]

[1, 2, 4, 5]Department of Physics, Acharya Nagarjuna University, Nagarjuna Nagar-522510, A.P., India

[3]Physics Division, Department of Basic Sciences & Humanities, GMR Institute of Technology, Rajam-532127, A.P., India

Abstract: ***A single phase white light emitting Dy^{3+} ions doped $NaCaAlPO_4F_3$ phosphor was synthesized via solid state reaction using flux. The obtained sample was characterized by powder X-ray diffraction (PXRD), Optical absorption, Photoluminescence (PL) and Fourier Transform Infrared Spectroscopy (FT-IR) techniques. From powder XRD data, the average crystallite size and structural parameters are evaluated. Absorption spectra shows absorption peaks corresponding to the transitions from the $^6H_{15/2}$ ground state to various excited energy levels. Transition probabilities, branching ratios and radiative lifetime were evaluated by using Judd–Ofelt analysis. Photoluminescence spectra shows three prominent emission bands centered at 480, 577 and 624 nm corresponding to the $^4F_{9/2} \rightarrow {}^6H_J$ (J = 15/2, 13/2 and 11/2) transitions respectively. From the emission transitions, stimulated emission cross-section (σ_e) and gain bandwidth (GBW) were predicted. The colorimetric parameters CIE coordinates, Correlated colour temperature (CCT) of the prepared phosphor understands the suitability of these material for white light generation. FT-IR spectrum exhibits the characteristic vibration bands of the prepared phosphor material.***

Keywords: Phosphor, Cell parameters, Optical absorption, Judd-Ofelt analysis, CIE coordinates, Photoluminescence

1. Introduction

As the driving force of the country's economy, energy is a fundamental factor to ensure the development of material civilization of modern society. In the light-emitting areas, researchers are looking for energy-efficient and environmental phosphors for solid-state lighting [1-3]. During the past few years, the topic of producing white light in a single-phase host has been the subject of much speculation by an increasing number of research groups because of the advantages of high color rendering index (CRI), tunable correlated color temperature (CCT) and pure Commission Internationale de I'Eclairage (CIE) chromaticity coordinates, as well as averting the re-absorption existing in red–green–blue (RGB) tricolor phosphors for application in white light-emitting diodes (W-LEDs) [4-6]. Now, there has been an extensive research on phosphor hosts with low phonon energy and high stability, which are ideal for doping rare earth ions as they reduce multiphonon de-excitation between rare earth ion energy levels and enhance the quantum efficiency of luminescent transitions [8]. Among various rare earth ions, Dy^{3+} is capable of emitting several interesting wavelengths between its f–f transitions, which are having potential applications in diversified fields. It plays a major role in the preparation of white light emitting phosphors due to two characteristic blue and yellow intense emission bands in the visible region corresponding to transitions $^4F_{9/2}$ - ^6H_J (J=15/2,13/2) [9-11]. To accomplish white light emission, optimization of local field environment around Dy^{3+} ions with a suitable yellow to blue (Y/B) intensity ratio is significant [12]. However, few works have been reported on Dy^{3+} doped phosphate based phosphors for white light emission. Shinde et al., reported luminescence studies on $Li_2Sr_2Al_2PO_4F_9:Dy^{3+}$ phosphor [13], photo-luminescence characteristics of Dy^{3+} doped $KLa(PO_3)_4$ phosphor reported by Chemingui et al., [14], Ratnam et al., reported white light emitting $NaCaPO_4:Dy^{3+}$ phosphor [15], Zhang et al., reported $KSrBP_2O_8:Dy^{3+}$ single phase white emitting phosphor by solid state reaction method [16].

At present, researchers explored an entirely new aluminate halophosphate based phosphor with structural diversity, chemical stability and high absorption yields [17]. Recently Shinde and co-workers reported various rare-earth halophosphates for lighting applications [13,18,19]. As a substantial host of luminescent material, $NaCaAlPO_4F_3$ is a halophosphate based phosphor and its crystal structure resembles with alumina fluorophosphate of sodium and calcium, named as Viitaniemiite, $NaCaAlPO_4(F,OH)_3$ reported by Ramik et al. This mineral belongs to monoclinic structure with the space group $P2_1/m$ [20, 21].

Recently authors reported the synthesis and characterization of transition ions and rare earth doped $NaCaAlPO_4F_3$ phosphor [22-26]. The present work reports studies made on structural and optical properties of Dy^{3+} ions doped $NaCaAlPO_4F_3$ phosphor by solid state reaction method. The present study is to perceive the crystal structure and evaluate the lattice cell parameters by powder X-ray diffraction, identify the local structural groups through FT-IR spectrum, determination of Judd–Ofelt parameters from the absorption spectra, which also provide us enough information for calculating the bonding (β and δ) parameters, analyzation of the photoluminescent spectrum to estimate radiative properties and life time and finally to explore the suitability of the prepared phosphor

towards white light application through colorimetric characterizations.

2. Experimental Section

2.1 Chemicals and Synthesis Procedure

Dy^{3+} ions doped $NaCaAlPO_4F_3$ phosphor was prepared by solid state reaction method. Sodium carbonate (Na_2CO_3), Calcium carbonate ($CaCO_3$), Diammonium hydrogen orthophosphate ($(NH_4)_2HPO_4$) were purchased from Sigma-Aldrich Corp., Aluminum tri fluoride ($AlF_3.3H_2O$) and Samarium oxide (Sm_2O_3) were purchased from Merck Chemicals. All of the chemical reagents used in this experiment were analytical grade and used without further purification.

The starting chemicals Na_2CO_3, $AlF_3.3H_2O$, $CaCO_3$, $(NH_4)_2HPO_4$ were weighed in a requisite stoichiometric proportion and ground into fine powder for 30 minutes using an agate mortar and pestle. After that Dy_2O_3 was added to the above mixture and grounded in an agate mortar for another one hour. The obtained chemical mixture was taken in a crucible for sintering at 650 $^{\circ}$C for 8 hours, 700°C for 4 hours, 750°C for 2 hours in a high temperature furnace with several intermediate grindings for 30 minutes and with excess of 20 mol% $AlF_3.3H_2O$ was also used as a flux finally to obtain Dy^{3+} ions doped $NaCaAlPO_4F_3$ phosphor.

The prepared phosphor was characterized by several techniques. X-ray diffraction (XRD) pattern of the prepared sample is recorded on Shimadzu-6100 with Cu K_α radiation. Optical absorption spectrum is recorded at room temperature on JASCO V670 spectrophotometer in the wavelength region of (200-1800) nm. Photoluminescence spectrum is recorded at room temperature on Horiba Jobin-Yvon Fluorolog-3 Spectrofluorimeter with Xe continuous (450 W) and pulsed (35 W) lamps as excitation sources. Shimadzu IR affinity FT-IR Spectrophotometer is used for recording of the prepared sample in the region 500–4000 cm^{-1}.

3. Results and Discussion

3.1 Powder X-ray diffraction Study

In order to determine the crystal structure, powder XRD analysis has been carried out. Figure 1 shows the X-Ray diffraction pattern of Dy^{3+} ions doped $NaCaAlPO_4F_3$ phosphor. The XRD pattern shows the peaks corresponding to the monoclinic structure. Nearly, all the diffraction peaks of the resultant phosphor is consistent with Joint Committee Powder Diffraction Standard data (JCPDS) file no 35-0598 and are well matched with those of the standard pattern of mineral Viitaniemiite [20].

The evaluated lattice cell parameters are: a = 0.6856, b = 0.7452 and c = 0.5523 nm, β = 109.68^0. These values are reliable with unit-cell parameters reported earlier [26].

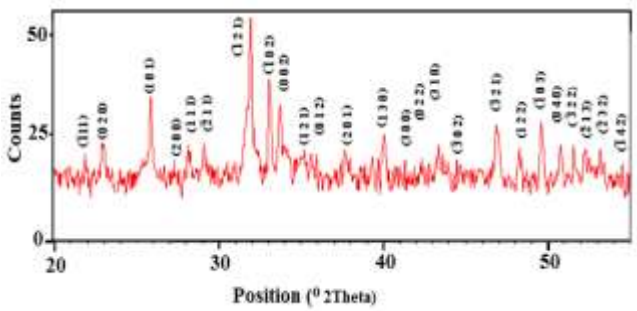

Figure 1: Powder X-ray diffraction pattern of Dy^{3+} ions doped $NaCaAlPO_4F_3$ phosphor.

From the XRD spectrum the average crystallite size was calculated from the most intense peak (1 2 1) using the Debye-Scherrer's formula [27],

$$d = (k\lambda / \beta \cos\theta)$$

where k = 0.89, λ represents the wavelength of Cu-Kα radiation, β is the full width at half maximum (FWHM) of the diffraction peak and θ is the angle of diffraction. Debye-Scherrer's formula is used to calculate the average crystallite size of Dy^{3+} doped phosphor and it is found to be 82 nm. The sharp and high intense peaks reveal that the prepared phosphor material is well crystalline material which can result in the high luminescence intensities.

3.2. Optical Absorption Spectra

3.2.1. Nephelauxetic ratio and bonding parameter

The optical absorption spectrum of Dy^{3+} ions doped $NaCaAlPO_4F_3$ phosphor sample in UV-VIS and NIR region is as shown in Figure 2 & 3. The absorptions bands were obtained at 27397, 26954, 26041, 23474, 22172, 20790, 14513, 12484, 11467, 9337, 7225 and 5787 cm^{-1}.

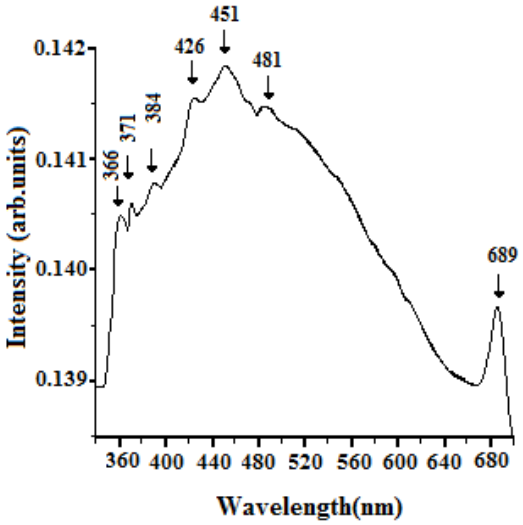

Figure 2: UV-Vis absorption spectrum of Dy^{3+} ions doped $NaCaAlPO_4F_3$ phosphor

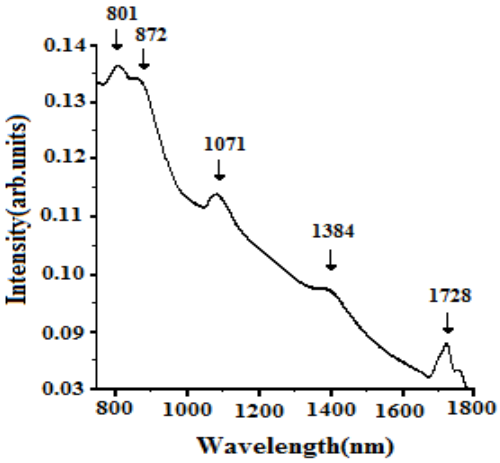

Figure 3: NIR absorption spectrum of Dy^{3+} ions doped $NaCaAlPO_4F_3$ phosphor.

The absorption bands correspond to the transitions that originate from the ground state $^6H_{15/2}$ to the excited states $^6P_{5/2}$, $^4M_{19/2}$, $^4F_{7/2}$, $^4G_{11/2}$, $^4I_{15/2}$, $^4F_{9/2}$, $^6F_{3/2}$, $^6F_{5/2}$, $^6F_{7/2}$, $^6F_{9/2}$, $^6F_{11/2}$ and $^6H_{11/2}$ respectively. The energy of these absorption transitions of Dy^{3+} ions in $NaCaAlPO_4F_3$ phosphor are also compared with aquo-ion system [28] and shown in Table 1.

Table 1: Observed band positions of Dy^{3+} ions doped $NaCaAlPO_4F_3$ phosphor (ν_c) and aquoion (ν_a) (cm^{-1}) along with nephelauxetic ratio (β) and bonding parameter (δ).

Transition $^6H_{15/2}$	ν_c (cm^{-1})	ν_a (cm^{-1})	β
$^6P_{5/2}$	27397	27400	0.999
$^4M_{19/2}$	26954	26400	1.020
$^4F_{7/2}$	26041	25800	1.009
$^4G_{11/2}$	23474	23400	1.003
$^4I_{15/2}$	22172	22100	1.003
$^4F_{9/2}$	20790	21100	0.985
$^6F_{3/2}$	14513	13250	1.095
$^6F_{5/2}$	12484	12400	1.006
$^6F_{7/2}$	11467	11000	1.042
$^6F_{9/2}$	9337	9100	1.026
$^6F_{11/2}$	7225	7730	0.934
$^6H_{11/2}$	5787	5850	0.989
β = 1.00925			
δ = -0.0091 (ionic bonding)			

The nature of the Dy^{3+} ligand bond can be understood by evaluating the nephelauxetic ratio (β) and bonding parameter (δ) [29]. The nephelauxetic ratio can be calculated by using the equation,

$$\beta = \nu_c/\nu_a$$

where ν_c and ν_a are the energies in cm^{-1} for a particular transition in the present host and aqueous solution [28] respectively. The bonding parameter can be evaluated by the equation,

$$\delta = (1-\beta')/\beta'$$

where β' is the average of the nephelauxetic ratios for all the observed transitions in the absorption spectrum. The nature of the ligand associated with Dy^{3+} in the host is revealed from the sign of the bonding parameter. The nephelauxetic ratios (β) and bonding parameter (δ) for the Dy^{3+} ions doped $NaCaAlPO_4F_3$ phosphor are presented in Table 1 and the nature of the Dy^{3+} ligand bond in the present host is found to be ionic.

3.2.2. Judd–Ofelt intensity parameters

The intensity of an absorption band is expressed in terms of "oscillator strength". The Judd-Ofelt theory has been applied to the absorption bands for Dy^{3+} ions doped $NaCaAlPO_4F_3$ phosphor recorded in the wavelength range 350–700 nm (UV-VIS) and 800–1800 nm (IR) as shown in Figure 2 & 3. The experimental oscillator strengths (f_{exp}) of absorption bands for Dy^{3+} ions doped $NaCaAlPO_4F_3$ phosphor are evaluated by measuring the integrated areas under the absorption bands using the relation [30],

$$f_{exp} = 4.32 \times 10^{-9} \int \varepsilon(\nu)\, d\nu$$

where ε(ν) represents the molar absorption coefficient of an absorption band at a wavenumber (cm^{-1}) and dν is the half-band width. According to J-O theory the calculated oscillator strength(f_{cal}) [31, 32] of an electric-dipole allowed transition J-J′ is given as,

$$f_{cal} = \frac{8\pi^2 mc\nu}{3h(2j+1)} \frac{(n^2+2)^2}{9n} \sum_{\lambda=2,4,6} \Omega_\lambda \left(< \psi J \,||\, U^\lambda \,||\, \psi' J' > \right)^2$$

where m represents the mass of an electron, h is the Plank's constant, ν is the mean energy of the transition, n is the refractive index of the sample, J and J′ are the total angular momentum for the ground and upper level respectively, Ω_λ are the J-O intensity parameters (Ω_2, Ω_4, Ω_6) that are characteristic of a given rare earth ion and $||U^{(\lambda)}||^2$ is the doubly reduced matrix elements of unit tensor operator evaluated in the intermediate coupling approximation for the absorption transition [28]. Considering the quite similar crystal structure between Vittanimite and $NaCaAlPO_4F_3$ phosphor host matrix, the refractive index of $NaCaAlPO_4F_3$ phosphor is assumed from Vittanimite and its value is 1.546 [20]. The f_{exp} values were evaluated from the absorption bands, whereas the f_{cal} values were calculated from the J-O theory. The J-O parameters are determined by least square fitting procedure and the reduced matrix elements, $||U^{(\lambda)}||^2$ (λ= 2, 4 and 6), were taken from Ref. [33].

The host dependent J-O intensity parameters (Ω_2, Ω_4, Ω_6), experimental (f_{exp}) and calculated (f_{cal}) oscillator strength of Dy^{3+} ions doped $NaCaAlPO_4F_3$ phosphor are presented in Table 2. Among the three J-O parameters, Ω_2 is more sensitive to the environment of the RE^{3+} ion and in turn strongly depends on hypersensitive transition. Ω_4 and Ω_6 are related to the long range effects and are strongly influenced by the vibrational levels associated with the central rare-earth ions bound to the ligand atoms. Generally, J-O parameters (Ω_2, Ω_4 and Ω_6) provide information about the nature of the metal–ligand bond and the symmetry around the site occupied by the RE ion in the host [34, 35].

From the table it is observed that $\Omega_2 > \Omega_6 > \Omega_4$ indicating the covalent nature of the bonding between the Dy^{3+} ions and the host. The similar trend of J-O parameters can be observed in different host matrices [36 - 39].

Table 2: Oscillator strengths and Judd-Ofelt parameters (Ω_2, Ω_4, Ω_6) of Dy^{3+} ions doped $NaCaAlPO_4F_3$ phosphor.

Transition $^6H_{15/2}$	ν (cm^{-1})	f_{exp}(X10^{-6})	f_{cal}(X10^{-6})	Δf(X10^{-6})
$^6P_{5/2}$	27397	1.2177	0.8563	0.3614
$^4M_{19/2}$	26954	0.8736	1.1920	0.3180
$^4F_{7/2}$	26041	1.1305	0.5560	0.5745
$^4G_{11/2}$	23474	0.6244	0.0524	0.5720
$^4I_{15/2}$	22172	0.6109	0.7128	0.1018
$^4F_{9/2}$	20790	3.9229	2.6346	1.2883
$^6F_{3/2}$	14513	0.6581	0.3683	0.2898
$^6F_{5/2}$	12484	0.7428	1.7932	1.0504
$^6F_{7/2}$	11467	0.9235	3.6136	2.6901
$^6F_{9/2}$	9337	2.4660	3.5026	1.0366
$^6F_{11/2}$	7225	3.1474	4.8458	1.6984
$^6H_{11/2}$	5787	2.6219	1.8420	0.7799

$\sigma_{rms} = 1.295 \times 10^{-6}$

$\Omega_2 = 5.405 \times 10^{-20}$, $\Omega_4 = 1.394 \times 10^{-20}$, $\Omega_6 = 4.437 \times 10^{-20}$

Higher value of Ω_2 indicates high degree of metal-ligand covalency bond and lower symmetry of the coordination structure surrounding the Dy^{3+} ions [40]. The value of Ω_2 for Dy^{3+} ions doped $NaCaAlPO_4F_3$ phosphor is found to be lower than that of Dy^{3+} ions doped phosphors [12,36,37,41], indicating less covalent nature. The evaluated J-O parameters, Ω_2, Ω_4, Ω_6 are presented in Table 3 along with those reported Dy^{3+} doped phosphors [36, 37].

Table 3: Comparison of J-O parameters (x10^{-20} cm^2) and their trend in Dy^{3+} doped phosphors

Phosphors	Ω_2	Ω_4	Ω_6	Trend
$NaCaAlPO_4F_3$ (Present)	5.40	1.39	4.43	$\Omega_2 > \Omega_6 > \Omega_4$
$CaMoO_4$ (1.5 mol %)[36]	9.58	1.89	4.78	$\Omega_2 > \Omega_6 > \Omega_4$
$CaMoO_4$ (2 mol %) [36]	7.21	1.41	3.59	$\Omega_2 > \Omega_6 > \Omega_4$
BiOCl (0.01 mol %)[37]	7.29	1.72	3.31	$\Omega_2 > \Omega_6 > \Omega_4$
BiOCl (0.03 mol %)[37]	7.51	1.83	3.49	$\Omega_2 > \Omega_6 > \Omega_4$

A measure of the accuracy of the fit between the experimental and calculated oscillator strengths is given by the root mean square (rms) deviation,

$$\delta_{rms} = \left[\frac{\sum(f_{exp} - f_{cal})^2}{N}\right]^{1/2}$$

where N is the number of levels included in the fit. The small deviation of rms value indicates a good fit between experimental and calculated oscillator strength as given in Table 2.

3.3 Photoluminescence spectrum

Under 380 nm excitation wavelength, the emission spectrum of Dy^{3+} ions doped $NaCaAlPO_4F_3$ phosphor exhibits sharp emission peaks centered at 450, 480, 514, 577 and 624 nm corresponding to $^4I_{15/2} \rightarrow {}^6H_{15/2}$ [14], $^4F_{9/2} \rightarrow {}^6H_{15/2}$, $^4I_{15/2} \rightarrow {}^6H_{13/2}$ [42], $^4F_{9/2} \rightarrow {}^6H_{13/2}$ and $^4F_{9/2} \rightarrow {}^6H_{11/2}$ due to the intra-configurationally ^4f - ^4f transitions of Dy^{3+} ions, as shown in Figure 4.

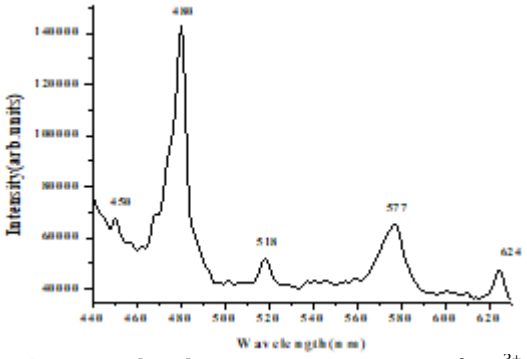

Figure 4: Photoluminescence spectrum of Dy^{3+} ions doped $NaCaAlPO_4F_3$ phosphor.

Among the transitions 480 and 577 nm are intense, a transition corresponding to (577 nm) $^4F_{9/2} \rightarrow {}^6H_{13/2}$ is in the yellow region and hyper sensitive obeying the selection rules $\Delta J = \pm 2$ and $\Delta L = \pm 2$ [43]. The yellow emission is related to the electric dipole (ED) transition, strongly influenced by the crystal-field environment. The transition corresponding to the (480 nm) $^4F_{9/2} \rightarrow {}^6H_{15/2}$ is in the blue region, which is a magnetic dipole (MD) transition less sensitive to the crystal fields.

The intensity ratio of the ED to MD transitions could be used to know the symmetry of the local environment of the f ions. The greater the intensity of ED transition indicates high asymmetry nature [44-46]. From Figure 4, it can be seen that the fluorescence intensity of the MD transition $^4F_{9/2} \rightarrow {}^6H_{15/2}$ possess higher intensity than the allowed ED transition $^4F_{9/2} \rightarrow {}^6H_{13/2}$ revealing a higher symmetry around the Dy^{3+} ions. Similar observations have also been reported in certain Dy^{3+} phosphor materials [47, 48]. In general the strong yellow emission decreases the color temperature of the phosphor and generates warm white light emission [49]. So the strong blue emission in Dy^{3+} ions doped $NaCaAlPO_4F_3$ phosphor is capable of generating a cool white light potential for solid state lighting.

3.4. Radiative parameters

The evaluated J-O intensity parameters are used to calculate the radiative parameters such as electric dipole line strength (S_{ed}), magnetic dipole line strength (S_{md}), radiative transitions probabilities (A_{ed} and A_{md}), spontaneous transition probabilities (A_R), total transition probability (A_T), radiative life time (τ_R) and branching ratios (β_R) corresponding to different emission channels from $^4F_{9/2} \rightarrow {}^6H_J$ (J = 15/2, 13/2 and 11/2) have also been calculated using the relations described elsewhere [50] and are presented in Table 4. Experimental branching ratios are the relative areas corresponding to different transitions. Branching ratio of each transition has been calculated from the luminescence spectra. The stimulated emission cross-section (σ_e) of each transition is found by using the equation, [51]

$$\sigma_e = \frac{\lambda_p{}^4}{8\pi c\, n^2 \Delta\lambda_{eff}} A_R\,(\Psi j; \Psi' j')$$

where λ_p is the peak wavelength of emission band, $\Delta\lambda_{eff}$ is full width at half maximum wavelength of the transition, n is the refractive index of the host and c is the light velocity. The values of stimulated emission cross-section indicate the rate of energy extraction from the phosphor material.

Table 4: Calculated dipole line strengths (S_{ed} and S_{md}x10^{-22}), Radiative transitions probabilities (A_{ed} and A_{md}), radiative lifetime ($\tau_R$ms) and branching ratios (β_R) of Dy^{3+} ions doped $NaCaAlPO_4F_3$ phosphor.

Transition S_{ed} $^4F_{9/2}$		S_{md}	A_{ed}	A_{md}	A_R	β_R
$^6H_{5/2}$	0.241	0	2.024	0	2.024	0.002
$^6H_{7/2}$	0.498	0.656	5.430	1.839	7.269	0.009
$^6F_{9/2}$	0.334	1.139	3.772	3.310	7.082	0.009
$^6F_{11/2}$	0.822	7.582	12.324	29.266	41.590	0.056
$^6H_{9/2}$	0.712	0.434	11.426	1.793	13.219	0.017
$^6H_{11/2}$	1.628	1.157	35.857	6.561	42.437	0.057
$^6H_{13/2}$	12.80	0	436.037	0	436.037	0.589
$^6H_{15/2}$	3.259	0	189.66	0	189.66	0.256

A_T = 739.320 s^{-1}, τ_R =1.352 ms

Experimental branching ratios and stimulated emission cross-sections of each transition obtained from the luminescence spectrum is reported in Table 5. It is observed that the calculated branching ratio (β_R), stimulated emission cross-section ($\sigma(\lambda_p)$) and GBW are found to be maximum for $^4F_{9/2} \rightarrow {}^6H_{13/2}$ transition. The experimental branching ratio (β_m) obtained from the relative area of emission bands characterizes the lasing strength and is found high for $^4F_{9/2} \rightarrow {}^6H_{15/2}$. As can be seen from Table 5, the experimental β_m follows the trend as $^6H_{11/2} < {}^6H_{13/2} < {}^6H_{15/2}$ where as calculated β_R follows $^6H_{11/2} < {}^6H_{15/2} < {}^6H_{13/2}$. The variation in radiative and experimental branching ratios may be due to the contribution of non-radiative processes from the $^4F_{9/2}$ level of Dy^{3+} ions in the prepared sample. Similar trend can be found in previous reports [52, 53]. It is observed that, the sum of the branching ratios of the $^4F_{9/2} \rightarrow {}^6H_{15/2}$ and $^4F_{9/2} \rightarrow {}^6H_{13/2}$ transitions are found to be approximately unity (~1) and is useful to achieve higher stimulated emission cross-section and quantum efficiency [54, 55].

Table 5: Emission peak wavelength ($\lambda_p$nm), Stimulated emission cross section ($\sigma(\lambda_p)$x10^{-22} cm^2) and (GBWx10^{-28} cm^3) and branching ratios (β_R and β_m) of Dy^{3+} ions doped $NaCaAlPO_4F_3$ phosphor.

Transition	λ_p	$\Delta\lambda_{eff}$	$\sigma(\lambda_p)$	GBW	β_m	β_R
$^6H_{15/2}$	480	83.14	24.260	55.89	0.718	0.256
$^6H_{13/2}$	577	105.68	80.317	266.47	0.240	0.589
$^6H_{11/2}$	624	40.41	9.173	35.72	0.041	0.057

3.5. Colorimetric performance

3.5.1. Color coordinates

The luminescence color of the samples excited under 380 nm has been characterized by the CIE (Commission International de I'Eclairage) 1931 chromaticity diagram [56]. The emission spectrum of the Dy^{3+} ions doped $NaCaAlPO_4F_3$ phosphor was converted to the CIE 1931 chromaticity diagram using the photo-luminescent data and the interactive CIE software (CIE coordinate calculator) as shown in Figure 5 [57].

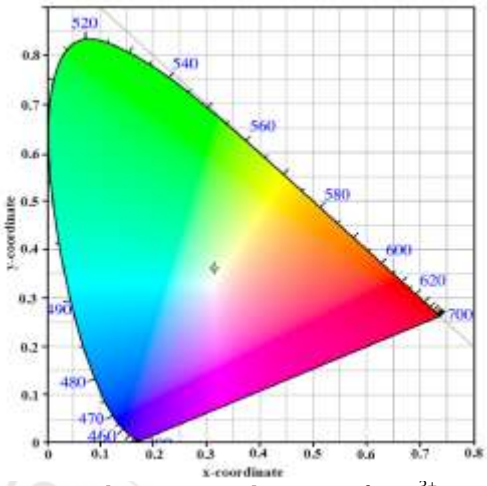

Figure 5: CIE chromaticity diagram of Dy^{3+} ions doped $NaCaAlPO_4F_3$ phosphor.

From Figure 5 it can be seen that the color coordinates of the Dy^{3+} ions doped $NaCaAlPO_4F_3$ phosphor lie in the white light region (0.325, 0.374) which is very near to "ideal white" (0.33, 0.33) in the chromaticity diagram. PL emission band positions and corresponding chromaticity coordinates of different white light emitting phosphors [58-61] are summarized in Table 6.

Table 6: Comparison of PL emission bands and corresponding chromaticity coordinates of different white light emitting phosphors.

Phosphor	Excitation Wavelength (nm)	Band Position (nm) Blue	Yellow	CIE coordinates x	y
$NaCaAlPO_4F_3$	380	480	577	0.325	0.374 (Present)
$NaSrB_5O_9$	390	482	582	0.299	0.299 [58]
$BaNb_2O_6$	386	482	472	0.322	0.339 [59]
BaY_2ZnO_5	355	480	579	0.320	0.389 [60]
$Sr_2MgSi_2O_7$	351	480	575	0.330	0.370 [61]

3.5.2. Correlated Color Temperature (CCT)

The correlated color temperatures (CCT) represents the quality of the light emitting source, which illustrates the temperature of a closest Planckian black-body radiator to the operating point on the chromaticity diagram [62]. CCT relates to the color of light produced by a light source, measured in degrees Kelvin. The CCT rating is an indication of how "warm" or "cool" the light source appears. The higher CCT value indicates the cool white light emission, where as in warm white emission the CCT value is low. However, opposite to the temperature scale, lamps with a CCT rating below 3200 K are usually considered as "warm" sources, while those with a CCT above 4000 K are considered as "cool" in appearance. McCamy has proposed the analytical equation to calculate the CCT [63], and is given by the expression,

$$CCT = -449\ n^3 + 3525\ n^2 - 6823n + 5520.33$$

where $n = (x - x_e)/(y - y_e)$ is the inverse slope line and (x_e = 0.332, y_e = 0.186) is the epicenter of the convergence. The CCT value of the prepared phosphor is found to be 5905 K, i.e. CCT > 4000 K. The CCT value lies in the cool white light region signifying the possibility of the prepared phosphor for the application in w-LEDs.

3.5.3. Colour purity

The color purity of the dominant emission is also important to realize better light source for LED applications and the color purity is calculated using the following equation

$$\text{colour purity} = \frac{\sqrt{(x - x_i)^2 + (y - y_i)^2}}{\sqrt{(x_d - x_i)^2 + (y_d - y_i)^2}}$$

where x_i and y_i are the chromaticity color coordinates corresponding to the equal energy point (0.33, 0.33) and (x_d, y_d) are the chromaticity color coordinates of the dominant wavelength point calculated from the intersection point of the connecting line between equal energy point (0.265, 0.723) and (x, y) = (0.325, 0.374) color coordinates in the chromaticity diagram [64]. The color purity is found to be 10.2 x 10^{-2}. The color purity should be very low to achieve white light emission from the emitting sources [52, 65] and the color purity for the standard white light is 0% [52, 66]. The color purity of the present sample is very closed to zero and well consistent with recently reported Dy doped hosts [52, 65,67], which indicates that the lower color purity of the Dy^{3+} ions doped $NaCaAlPO_4F_3$ phosphor is suitable for the generation of white light and further suggest their utility and suitability for W-LED applications.

3.6. FT-IR study

Figure 6 presents the FTIR spectrum of Dy^{3+} ions doped $NaCaAlPO_4F_3$ phosphor exhibiting several transmission bands at 3177, 1654, 1583, 1399, 756 and 894 cm^{-1}. The assignments of the peak position and their bonding are given in Table 7. The vibrational modes of hydroxyl ions are observed in the region of 4000-3000 cm^{-1}. In IR spectrum of the prepared phosphor, broad band at 3177 cm^{-1} affirms the symmetric and asymmetric modes of hydroxyl (O–H) groups. Vibrational modes of P-O-H are observed at 1654 and 1583 cm^{-1} [68]. Asymmetric modes of O-P-O are detected at 1399 cm^{-1} [69]. The stretching vibrations of F-P-F are perceived at 756 and 894 cm^{-1} which specify the formation of F-P-F bonds and their existence as fluorophosphates units [70]. All the assignments made for phosphor is found to be comparable to the literature reported earlier [22].

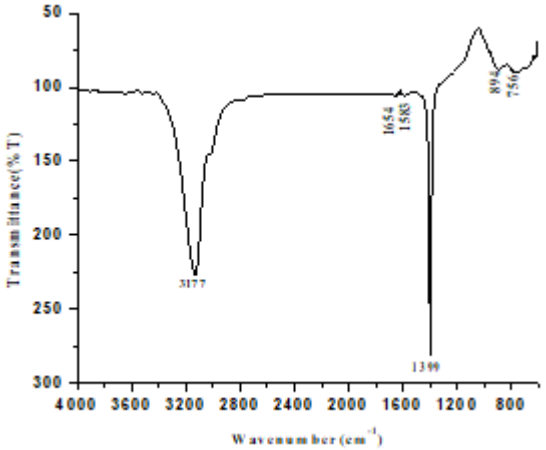

Figure 6: FT-IR spectrum of Dy^{3+} ions doped $NaCaAlPO_4F_3$ phosphor

Table 7: Assignments of vibrational bands in FT-IR spectrum of Dy^{3+} ions doped $NaCaAlPO_4F_3$ phosphor

Vibrational frequency (cm^{-1})	Band assignment
3177	Symmetric and asymmetric modes of vibrations of hydroxyl ions
1654, 1583	P-O-H modes of vibrations
1399	asymmetric mode of O-P-O
894,756	Stretching vibrations of F-P-F

4. Conclusion

In summary, the structural and luminescent properties of single phase white light emitting Dy^{3+} ions doped $NaCaAlPO_4F_3$ phosphor was synthesized by the solid-state reaction method. X-ray diffraction (XRD) pattern confirms the monoclinic structure and crystallinity of the sample. The nephelauxetic ratio and bonding parameters calculated through the optical absorption spectra suggests the ionic character of the Dy^{3+} ions with its surrounding ligands. The J-O parameters of the Dy^{3+} ions doped $NaCaAlPO_4F_3$ phosphor followed the trend $\Omega_2 > \Omega_6 > \Omega_4$. Photoluminescence spectrum under the ultraviolet (UV) excitation at 380 nm, exhibits three characteristic luminescent peaks at 480 nm blue emission ($^4F_{9/2} \rightarrow {}^6H_{15/2}$), the 577 nm yellow emission ($^4F_{9/2} \rightarrow {}^6H_{13/2}$) and the 624 nm red emission ($^4F_{9/2} \rightarrow {}^6H_{11/2}$). The fluorescence intensity of the $^4F_{9/2} \rightarrow {}^6H_{15/2}$ transition possess higher intensity than the allowed $^4F_{9/2} \rightarrow {}^6H_{13/2}$ transition revealing a higher symmetry around the Dy^{3+} ions. The branching ratios calculated from J-O theory are found to be in small deviation with experimental values due to the contribution of non-radiative processes. The CIE color coordinates were calculated from emission spectrum and found to be located in white region (0.325, 0.374). The color purity (10.2 x 10^{-2}) and CCT (5905 K) of the sample indicates the emission of cool white light from Dy^{3+} ions doped $NaCaAlPO_4F_3$ phosphor. The FT-IR spectrum confirms the formation of PO_4 groups. The evaluated luminescent properties reveal the feasibility of Dy^{3+} ions doped $NaCaAlPO_4F_3$ phosphor for the production of white light emitting diodes.

5. Acknowledgements

RVSSN would like to thank the University Grants Commission-DSA1 and DST-FIST, New Delhi for sanctioning to the Department of Physics, Acharya Nagarjuna University to carry out the present research work.

References

[1] Q. Zhang, C.F. Wang, L.T. Ling, S. Chen, "Fluorescent nanomaterial-derived white light-emitting diodes: what's going on", J. Mater. Chem. C, 2, pp. 4358- 4373, 2014.
[2] C. Shen, Y. Yang, S. Jin, J. Ming, H. Feng, Z. Xu, "White light-emitting diodes using blue and yellow–orange-emitting phosphors", Optik, 121, pp. 1487-1491, 2010.
[3] R. Wang, J. Xu, C. Chen, "Luminescent characteristics of $Sr_2B_2O_5$: Tb^{3+}, Li^+ green phosphor", Mater. Lett., 68, pp. 307-309, 2012.
[4] M. Shang, C. Li, J. Lin, "How to produce white light in a single-phase host?", Chem. Soc. Rev., 43, pp. 1372-1386, 2014.
[5] H. Liu, L. Liao, M.S. Molokeev, Q. Guo, Y. Zhang, L. Mei, "A novel single-phase white light emitting phosphor $Ca_9La(PO_4)_5(SiO_4)F_2$:Dy^{3+}: synthesis, crystal structure and luminescence properties", RSC Adv., 6, 24577-24583, 2016.
[6] A.J. Fernández-Carrión, M. Ocaña, J. García-Sevillano, E. Cantelar, A.I. Becerro, "New Single-Phase, White-Light-Emitting Phosphors Based on δ-$Gd_2Si_2O_7$ for Solid-State Lighting", J. Phys. Chem. C, 118, pp. 18035-18043, 2014.
[7] B. Yan, C. Wang, "Synthesis and luminescence properties of $REAl_3(BO_3)_4$:Eu^{3+}/Tb^{3+} (RE = Y, Gd) phosphors from sol–gel composition of hybrid precursors", Solid State Sci., 10, pp. 82-89, 2008.
[8] R. Shrivastava, J. Kaur, V. Dubey, "White Light Emission by Dy^{3+} Doped Phosphor Matrices: A Short Review", J. Fluoresc., 26, pp. 105-111, 2016.
[9] R. Yu, D.S. Shin, K. Jang, Y. Guo, H.M. Noh, B.K. Moo, B.C. Choi, J.H. Jeong, S.S. Yi, "Luminescence and thermal-quenching properties of Dy^{3+}-doped Ba_2CaWO_6 phosphors", Spectrochim. Acta A, 125, pp. 458-462, 2014.
[10] Z. Li, H.G. Cai, "Novel Dy^{3+}-doped $Gd(PO_3)_3$ white-light phosphors under VUV excitation for Hg-free lamps application", Chin. Phys. B, 22, pp. 027803-0278038, 2013.
[11] B. Liu, C. Shi, "Potential white-light long-lasting phosphor: Dy^{3+}-doped aluminate", Appl. Phys. Lett., 86, pp. 191111-191116, 2005.
[12] K. Linganna, C.S. Rao, C.K. Jayasankar, "Optical properties and generation of white light in Dy^{3+}-doped lead phosphate glasses", J. Quant. Spectrosc. RA, 118, pp. 40-48, 2013.
[13] K.N. Shinde, S.J. Dhoble, "Luminescence in $Li_2Sr_2Al_2PO_4F_9$:Dy^{3+}- a novel nanophosphor", Lumin., 27, pp. 91-94, 2012.
[14] S. Chemingui, M. Ferhin, K. Horchani-Naifer, M. Férid, "Synthesis and luminescence characteristics of Dy^{3+} doped $KLa(PO_3)_4$", J. Lumin., 166, pp. 82-87, 2015.
[15] B.V. Ratnam, M. Jayasimhadri, K. Jang, H.S. Lee, S.-S.Yi, J.-H. Jeong, "White Light Emission from $NaCaPO_4$:Dy^{3+} Phosphor for Ultraviolet-Based White Light-Emitting Diodes", J. Am. Ceram. Soc., 93, pp. 3857-3861, 2010.
[16] F. Zhang, T. Zhang, G. Li, W. Zhang, "Single phase M^+(M = Li, Na, K), Dy^{3+} co-doped $KSrBP_2O_8$ white light emitting phosphors", J. Alloy. Comp., 618, pp. 484-487, 2015.
[17] Z. Yang, Z. Zhao, Y. Wen, Y. Wang, "Structure and luminescence properties of Bi^{3+} activated $Ca_{12}Al_{14}O_{32}Cl_2$ phosphors", J. Alloy. Comp., 559, pp. 142-145, 2013.
[18] K.N. Shinde, S.J. Dhoble, "Influence of Li^+ doping on photoluminescence properties of $Sr_5(PO_4)_3F$: Eu^{3+}", Adv. Mat. Lett., 1, pp. 254-258, 2010.
[19] S.J. Dhoble, K.N. Shinde, "Ce^{3+} and Eu^{3+} activated $Na_2Sr_2Al_2PO_4F_9$ nanophosphor", Adv. Mat. Lett., 2, pp. 349-353, 2011.
[20] R.A. Ramik, B.D. Sturman, A.C. Roberts, P.J. Dunn, "Viitaniemiite from the Francon Quarry, Montreal, Quebec", Can. Mine., 21, pp. 499-502, 1983.
[21] A. Pajunen, S.I. Lahti, "The crystal structure of Viitaniemiite, Locality: Viitaniemi pegmatite, Orivesi, southern Finland", Ameri. Miner., 69, pp. 961-966, 1984.
[22] V. Pushpa Manjari, Ch. Rama Krishna, Ch. Venkata Reddy, Sk. Muntaz Begum, Y.P. Reddy, R.V.S.S.N. Ravikumar, "Synthesis and characterization of undoped and Fe(III) ions doped $NaCaAlPO_4F_3$ phosphor", J. Lumin., 145, pp. 324-329, 2014.
[23] V. Pushpa Manjari, Ch. Rama Krishna, Sk. Muntaz Begum, R.V.S.S.N. Ravikumar, "Synthesis and spectral investigations of Mn(II) ions doped $NaCaAlPO_4F_3$ phosphor", Eur. Phys. J. Appl. Phys., 65, pp. 10403-10410, 2014.
[24] V. Pushpa Manjari, T. Aswani, B. Babu, G. Thirumala Rao, R. Joyce Stella, B. Jayaraja, R.V.S.S.N. Ravikumar, "EPR and Optical Studies of Cr(III) Ions Doped $NaCaAlPO_4F_3$ Nano Phosphor", Int. J. Cur. Engg. Tech., Special Issue-2, pp. 259-264, 2014.
[25] V. Pushpa Manjari, Ch. Rama Krishna, Ch. Venkata Reddy, R.V.S.S.N. Ravikumar, "Synthesis and spectral investigations of Cu(II) ions doped $NaCaAlPO_4F_3$ phosphor", Lumin., 29, pp. 1123-1129, 2014.
[26] R. Nagaraja, V. Pushpa Manjari, B. Sailaja, R.V.S.S.N. Ravikumar, "A novel orange emitting Sm^{3+} ions doped $NaCaAlPO_4F_3$ phosphor: Optical and luminescence properties", J. Mol. Struc., 1130, pp. 96-102, 2017.
[27] P. Klug, L.E. Alexander, X-ray Diffraction Procedure, Wiley, New York, 1954.
[28] W.T. Carnall, P.R. Fields, K. Rajnak, "Electronic Energy Levels in the Trivalent Lanthanide Aquo Ions Pr^{3+}, Nd^{3+}, Pm^{3+}, Sm^{3+}, Dy^{3+}, Ho^{3+}, Er^{3+} and Tm^{3+}", J. Chem. Phys., 49, pp. 4424-4442, 1968.

[29] S.P. Sinha, Complexes of the Rare Earths, Pergamon, Oxford, 1966.
[30] [30] W.T. Carnall, Non-metallic compounds. In: Gschneidner Jr. KA, Eyring L, Editors. Hand book on the physics and chemistry of rare earths, Amsterdam: North-Holland Publishing Co, vol. 3, pp. 171-208, 1979.
[31] B.R. Judd, "Optical absorption intensities of rare-earth ions", Phys. Rev., 127, pp. 750-761, 1962.
[32] G.S. Ofelt, "Intensities of crystal spectra of rare-earth ions", J. Chem. Phys., 37, pp. 511-520, 1962.
[33] C.K. Jayasankar, E. Rukmini, "Spectroscopic investigations of Dy^{3+} ions in borosulphate glasses", Phys. B, 240, pp. 273-288, 1997.
[34] S. Surendra Babu, P. Babu, C.K. Jayasankar, Th. Troster, S.W.G. Wortmann, "Optical properties of Dy^{3+}-doped phosphate and fluorophosphate glasses", Opt. Mater., 31, pp. 624-629, 2009.
[35] M. Jayasimhadri, L.R. Moorthy, K. Kojima, K. Yamamoto, N. Wada, "Optical properties of Dy^{3+} ions in alkali tellurofluorophosphate glasses for laser materials", J. Phys. D: Appl. Phys., 39, pp. 635-640, 2006.
[36] S. Dutta, S. Som and S. K. Sharma, "Excitation spectra and luminescence decay analysis of K^+ compensated Dy^{3+}doped $CaMoO_4$ phosphors", RSC Adv., 5, 7380-7387, 2009.
[37] C. Shivakumara, Rohit Saraf, Pramod Halappa, "White luminescence in Dy^{3+} doped BiOCl phosphors and their Judd–Ofelt analysis", Dyes Pigments,126, pp. 154-164, 2016.
[38] C.R. Kesavulu, C.K. Jayasankar, "White light emission in Dy^{3+}-doped lead fluorophosphate glasses", Mater. Chem. Phys., 130, pp. 1078-1085, 2011.
[39] A. Amarnath Reddy, M. Chandra Sekhar, K. Pradeesh, S. Surendra Babu, G. Vijaya Prakash, "Optical properties of Dy^{3+}-doped sodium–aluminum–phosphate glasses", J. Mater. Sci., 46, pp. 2018-2023, 2011.
[40] W.W. Zhou, B. Wei, W. Zhao, G.F. Wang, X. Bao, Y.H. Chen, F.W. Wang, J.M. Du, H.J. Yu, "Intense yellow emission in Dy^{3+}-doped $LiGd(MoO_4)_2$ crystal for visible lasers", Opt. Mater., 34, pp. 56-60, 2011.
[41] R. Praveena, R. Vijaya, C.K. Jayasankar, "Photoluminescence and energy transfer studies of Dy^{3+}-doped fluorophosphate glasses", Spectrochim. Acta A, 70, pp. 577-586, 2008.
[42] W.T. Carnall, "The absorption and fluorescence spectra of rare earth ions in solution", Handbook on the physics and chemistry of rare earths, Elsevier BV, Amsterdam, vol 3, Ch. 24, 1979.
[43] A. Mohan Babu, B.C. Jamalaiah, J. Suresh Kumar, T. Sasikala, L. Rama Moorthy, "Spectroscopic and photoluminescence properties of Dy^{3+}-doped lead tungsten tellurite glasses for laser materials", J. Alloys Compd., 509, pp. 457-462, 2011.
[44] Y. Gao, Q.H. Nie, T.F. Xu, X. Shen, Spectrochim. Acta A, 61, pp. 2822-2827, 2005.
[45] V. Uma, K. Maheshvaran, K. Marimuthu, G. Muralidharan, "Structural and optical investigations on Dy^{3+}doped lithium tellurofluoroborate glasses for white light applications", J. Lumin., 176, pp. 15-24, 2016.
[46] A. Balakrishna, D. Rajesh, Y.C. Ratnakaram, "Structural and photoluminescence properties of Dy^{3+}doped different modifier oxide-based lithium borate glasses", J. Lumin., 132, pp. 2984-2991, 2012.
[47] S. Selvi, G. Venkataiah, S. Arunkumar, G. Muralidharan, K. Marimuthu, "Structural and luminescence studies on Dy^{3+} doped lead boro–telluro-phosphate glasses", Phys. B, 454, pp. 72-81, 2014.
[48] A.N. Yerpude, S.J. Dhoble, "Synthesis and photoluminescence properties of Dy^{3+}, Sm^{3+} activated $Sr_5SiO_4Cl_6$ phosphor", J. Lumin., 132, pp. 2975-2978, 2012.
[49] I.P. Sahu, P. Chandrakar, R.N. Baghel, D.P. Bisen, N. Brahme, R.K. Tamrakar, "Luminescence properties of dysprosium doped calcium magnesium silicate phosphor by solid state reaction method", J. Alloys Compd., 649, pp. 1329-1338, 2015.
[50] B. Sailaja, R.J. Stella, G. Thirumala Rao, B. Jayaraja, V. Pushpa Manjari, R.V.S.S.N. Ravikumar, "Physical, structural and spectroscopic investigations of Sm^{3+} doped ZnO mixed alkali borate glass", J. Mol. Struct., 1096, pp. 129-135, 2015.
[51] P. Babu, H. Seo, C.R. Kesavulu, Y. Jang, C.K. Jayasankar, "Thermal and optical properties of Er^{3+}-doped oxyfluorotellurite glasses", J. Lumin., 129, pp. 444-448, 2009.
[52] N. Vijaya, K.U. Kumar, C.K. Jayasankar, "Dy^{3+}-doped zinc fluorophosphate glasses for white luminescence applications", Spectrochim. Acta A, 113, pp. 145-153, 2013.
[53] Sk. Nayab Rasool, L. Rama Moorthy, C.K. Jayasankar, "Optical and luminescence properties of Dy^{3+} ions in phosphate based glasses", Solid State Sci., 22, pp. 82-90, 2013.
[54] O. Ravi, C. Madhukar Reddy, B. Sudhakar Reddy, B. Deva Prasad Raju, "Judd–Ofelt analysis and spectral properties of Dy^{3+} ions doped niobium containing tellurium calcium zinc borate glasses", Opt. Comm., 312, pp. 263-268, 2014.
[55] R.J. Amjad, M.R. Sahar, S.K. Ghoshal, M.R. Dousti, R. Arifin, "Synthesis and characterization of Dy^{3+} doped zinc–lead-phosphate glass", Opt. Mater., 35, pp. 1103-1108, .
[56] G.B. String Fellow, M.G. Craford (eds.), "High Brightness Light Emitting Diodes in Semiconductors and Semi Metals", Academic Press, San Diego, vol. 48, 1997.
[57] CIE 1931, International Commission on Illumination, Publication CIE no. 15, (E-1.3.1) 1931
[58] G.R. Dillip, B. Ramesh, C.M. Reddy, K. Mallikarjuna, O. Ravi, S.J. Dhoble, S.W. Joo, B.D.P. Raju, "X-ray analysis and optical studies of Dy^{3+} doped $NaSrB_5O_9$ microstructures for white light generation", J. Alloys Compd., 615 pp. 719-727, 2014.
[59] A.K. Vishwakarma, J. Kaushal, M. Jayasimhadri, B. Sivaiah, G. Bhasker, D. Haranath, "Emerging cool white light emission from Dy^{3+} doped single phase alkaline earth niobate phosphors for indoor lighting applications", Dalton Trans., 44, 17166-17174, 2015.

[60] C.H. Liang, L.G. Teoh, K.T. Liu, Y.S. Chang, "Near white light emission of BaY_2ZnO_5 doped with Dy^{3+}ions", J. Alloys Compd., 517, pp. 9-13, 2012.
[61] B. Liu, L. Kong, C. Shi, "White-light long-lasting phosphor $Sr_2MgSi_2O_7:Dy^{3+}$", J. Lumin., 122-123, 121-124, 2007.
[62] T. Erdem, S. Nizamoglu, X.W. Sun, H.V. Demir, "A photometric investigation of ultra-efficient LEDs with high color rendering index and high luminous efficacy employing nanocrystal quantum dot luminophores", Opt. Express, 18, pp. 340-347, 2010.
[63] C.S. McCamy, "Correlated color temperature as an explicit function of chromaticity coordinates", Color Res. Appl., 17, pp. 142-144, 1992.
[64] E.F. Schubert, Light Emitting Diodes, second ed., Cambridge University Press, New York, pp. 292-310, 2006.
[65] K.V. Krishnaiah, K.U. Kumar, C.K. Jayasankar, "Spectroscopic properties of Dy^{3+}-doped oxyfluoride glasses for white light emitting diodes", Mater. Exp., 3, pp. 61-70, 2013.
[66] S. Arunkumar, G. Venkataiah, K. Marimuthu, "Spectroscopic and energy transfer behavior of Dy^{3+} ions in B_2O_3-TeO_2-PbO-PbF_2-Bi_2O_3-CdO glasses for laser and WLED applications", Spectrochim. Acta A, 136, pp. 1684-1697, 2015.
[67] K. Jha, M. Jayasimhadri, "Spectroscopic investigation on thermally stable Dy^{3+} doped zinc phosphate glasses for white light emitting diodes", J. Alloys Compd., 688, pp. 833-840, (2016).
[68] G.R. Hunt, J.W. Salisbury, J.C. Lenhoff, "Visible and near infrared spectra of minerals and rocks: V. Halides, arsenates, vanadates, and borates", Mode. Geol., 3, pp. 121-132, 1972.
[69] K. Swapna, Sk. Mahamuda, A. Srinivasa Rao, M. Jayasimhadri, T. Sasikala, L. Rama Moorthy, "Optical absorption and luminescence characteristics of Dy^{3+} doped Zinc Alumino Bismuth Borate glasses for lasing materials and white LEDs", J. Lumin., 139, pp. 119-124, 2013.
[70] K. Nakamoto, IR and Raman spectra of Inorganic and Coordination Compounds, 4th Ed., Wiely, Newyork, 1986